Rain Initiation Time in Turbulent Warm Clouds

GREGORY FALKOVICH AND MIKHAIL G. STEPANOV

Institute for Advanced Study, Princeton, New Jersey, and Weizmann Institute of Science, Rehovot, Israel

MARIJA VUCELJA

University of Belgrade, Belgrade, Serbia and Montenegro, and Weizmann Institute of Science, Rehovot, Israel

(Manuscript received 19 November 2004, in final form 25 August 2005)

ABSTRACT

A mean field model is presented that describes droplet growth resulting from condensation and collisions and droplet loss resulting from fallout. The model allows for an effective numerical simulation. The numerical scheme that is conservative in water mass and keeps accurate count of the number of droplets is applied, and the way in which the rain initiation time depends on different parameters is studied. In particular, it is shown that the rain initiation time depends nonmonotonically (has a minimum) on the number of cloud condensation nuclei. Also presented is a simple model that allows one to estimate the rain initiation time for turbulent clouds with an inhomogeneous concentration of cloud condensation nuclei. It is argued that by overseeding even a part of a cloud by small hygroscopic nuclei one can substantially delay the onset of precipitation.

1. Introduction

In warm clouds, droplets grow by vapor condensation on cloud condensation nuclei (CCN) and by coalescence resulting from collisions until the raindrops fall out of the cloud—see, for example, Pruppacher and Klett (1997). Those processes can be modeled by the equation for the local distribution of droplets over sizes $n(a, t, \mathbf{r}) = n(a)$ and the water vapor density $M(t, \mathbf{r})$:

$$\frac{\partial n(a)}{\partial t} + (\mathbf{v}\cdot\nabla)n = -ks\frac{\partial}{\partial a}\frac{n(a)}{a} + \int da'\left[\frac{K(a', a'')n(a')n(a'')}{2(a''/a)^2} - K(a', a)n(a')n(a)\right] \tag{1}$$

and

$$\frac{\partial M}{\partial t} + (\mathbf{u}\cdot\nabla)M - \kappa\nabla^2 M = -4\pi s M\kappa\int an(a)\,da. \tag{2}$$

See Table 1 for definitions of variables. The first term in the right-hand side of (1) is because of condensation, which changes the droplet size a according to $da^2/dt = 2ks$, where s is supersaturation and the effective diffusion rate k (depending on M) is given by (13.28) from Pruppacher and Klett (1997): $k^{-1} = \kappa^{-1}(\rho_0/M) + \kappa_T^{-1}(\mathcal{L}\mathcal{M}_w/RT)^2$. Here, κ is vapor diffusivity and κ_T is thermal conductivity, L is the latent heat of condensation, $\mathcal{M}_w$ is the molecular weight of water, R is molar gas constant, and $\rho_0 = 1$ g cm^{-3} is the density of liquid water. This equation for the condensational droplet growth neglects curvature and solute effects, which is valid for sufficiently large droplets (over 1 μm). The second term in the rhs of (1) describes coalescence resulting from collisions—here $a'' = (a^3 - a'^3)^{1/3}$ is the size of the droplet that produces the droplet of size a upon coalescence with the droplet of size a'. The collision kernel is the product of the target area and the relative velocity of droplets upon the contact: $K(a, a') \simeq \pi(a + a')^2\Delta\upsilon$. According to the recent precise measurements (Beard et al. 2002), the coalescence efficiency of the droplets in the relevant intervals is likely to be greater than 0.95; we put it as unity in our calculations.

To describe the nine unknown functions, n, M, s, $\mathbf{v}$, and $\mathbf{u}$, one must also add the equation that describes the temperature change (that determines s) and Navier–

Corresponding author address: G. Falkovich, Physics of Complex Systems, Weizmann Institute of Science, Rehovot 76100, Israel.
E-mail: gregory.falkovich@weizmann.ac.il

TABLE 1. Definitions of variables.

Quantity	Units	Description
$n(a)$	cm^{-4}	Distribution of droplet sizes in a unit volume
P	cm	Mean radius of the initial distribution $n(a)$
σ	cm	Width of the initial distribution $n(a)$
a	cm	Droplet radius
$\mathbf{r}$	cm	Spatial coordinate
t	s	Time
W	No.	Fraction of water left in the cloud
t_*	s	Rain initiation time
K	$\text{cm}^3\,\text{s}^{-1}$	Collision kernel
$\mathbf{u}$	$\text{cm}\,\text{s}^{-1}$	Air velocity
$\mathbf{u}_g$	$\text{cm}\,\text{s}^{-1}$	Terminal fall velocity
$\mathbf{v}$	$\text{cm}\,\text{s}^{-1}$	Cloud particle velocity
g	$\text{cm}\,\text{s}^{-2}$	Acceleration of gravity
ν	$\text{cm}^2\,\text{s}^{-1}$	Air viscosity
ρ	$\text{g}\,\text{cm}^{-3}$	Air density
ρ_0	$\text{g}\,\text{cm}^{-3}$	Liquid water density
L	cm	Cloud vertical size
L	$\text{J}\,\text{mol}^{-1}$	Latent heat of condensation
M	$\text{g}\,\text{cm}^{-3}$	Water vapor density
κ	$\text{cm}^2\,\text{s}^{-1}$	Water vapor diffusivity
κ_T	$\text{cm}^2\,\text{s}^{-1}$	Thermal conductivity

Stokes equations for the cloud particle and air velocity. Such a system cannot be possibly solved numerically with any meaningful resolution, neither presently nor in a foreseeable future. The main problem is a very complicated spatial structure of the fields involved, particularly resulting from cloud turbulence. Our aim in this paper is to formulate some mean field model that does not contain spatial arguments at all. The requirements to this model are that it must give the correct qualitative relations between the parameters and a reasonable quantitative description (at least within the order of magnitude) of the real-world time scales. We use the model to study the evolution of $n(a, t)$ starting from micrometer sizes all the way to the moment when droplet fallout significantly decreases the water content in the cloud. We shall call this moment the rain initiation time, and we study how that time depends on initial vapor content and CCN concentration.

Beyond the scope of our model are effects related to spatial inhomogeneities and fluctuations of the fields. According to the two basic phenomena involved (condensation and collisions), the main effects are (i) the mixing and diffusion of water vapor, heat, and droplets, and (ii) the influence of cloud turbulence on collisions. We briefly address the first phenomenon in section 4, considering inhomogeneously seeded clouds. We do not consider here the controversial subject of collision enhancement by turbulence, giving instead in section 3 references to the relevant literature.

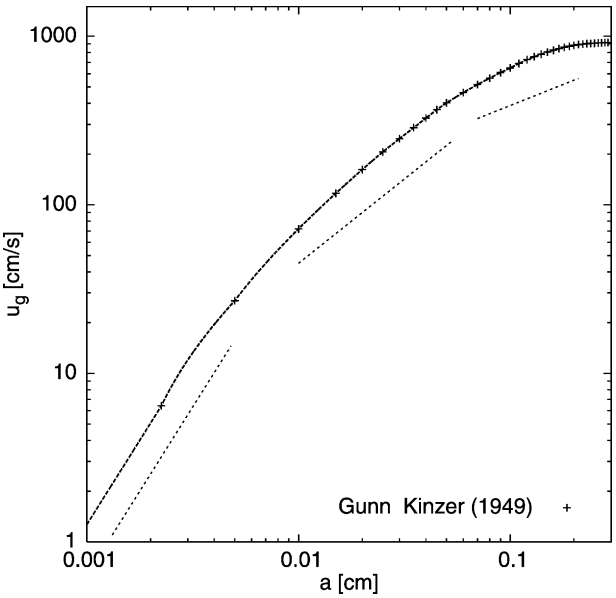

FIG. 1. Terminal fall velocity $\mathbf{u}_g$ as a function of cloud droplet radius a.

2. Growth by gravitational collisions

For the parameters typical for warm precipitating clouds [$sM/\rho_0 = 10^{-8}$–10^{-9} and $10^6 < n = \int n(a)\,da < 10^9\ \text{m}^{-3}$], collisions are negligible for micron-sized droplets (Pruppacher and Klett 1997). For droplets larger than 2 μm, Brownian motion can be neglected and the collision kernel in still air is due to gravitational settling:

$$K_g(a, a') = \pi(a + a')^2 E(a, a')|\mathbf{u}_g(a) - \mathbf{u}_g(a')|. \quad (3)$$

The fall velocity $\mathbf{u}_g$ is obtained from the balance of gravity force $4\pi g\rho_0 a^3/3$ and the drag $F(\mathbf{u}_g, a)$. The drag force depends on the Reynolds number of the flow around the droplet, $\text{Re}_a \equiv \mathbf{u}_g a/\nu$. When Re_a is of an order of unity or less, $F = 6\pi\nu\rho a\mathbf{u}_g$ and $\mathbf{u}_g = g\tau$, where ρ is the air density and $\tau = (2/9)(\rho_0/\rho)(a^2/\nu)$ is called Stokes time. We use $\mathbf{u}_g = g\tau$ for $a < 40$ μm and take $\mathbf{u}_g(a)$ from the measurements of Gunn and Kinzer (1949) for $a > 50$ μm with a smooth interpolation for 40 μm $< a <$ 50 μm, as shown in Fig. 1. The dotted straight lines have slopes 2, 1, and 1/2. One can see that $\mathbf{u}_g \propto a^2$ at $a < 40$ μm. There is an intermediate interval with an approximately linear law $\mathbf{u}_g \propto a$ for 40 μm $< a <$ 400 μm. When $\text{Re}_a \gg 1$ one may expect $F \propto \rho a^2 \mathbf{u}_g^2$, as long as the droplet remains spherical; that gives $\mathbf{u}_g \propto \sqrt{ag\rho_0/\rho}$. Square root law can be distinguished between 400 μm and 1 mm, while the growth of $\mathbf{u}_g(a)$ saturates at larger a because of shape distortions. Hydrodynamic interaction between approaching droplets

is accounted in K_g by the collision efficiency E, values for which we take from Pinsky et al. (2001) at the 750-hPa altitude.

It is of practical use to be able to predict the time left before rain starts given the knowledge of droplet distribution at a given instant. Such distributions can be measured with high accuracy by optical and other methods. Drop size distributions measured in many different types of clouds under a variety of meteorological conditions often exhibit a characteristic shape (Pruppacher and Klett 1997). Generally, the concentration rises sharply from a low maximum value, and then decreases gently toward larger sizes, causing the distribution to be positively skewed with a long tail toward the larger sizes. We approximate such a shape with half-Gaussian $n(a, 0) = \theta(a - a_0) \exp[-(a - a_0)^2/2\alpha^2]$, where θ is a step function. We thus characterize the initial distribution by two parameters: the first moment $P = \int an(a, 0)\, da/n$ (mean radius) and the width σ [$\sigma^2 = \int a^2 n(a, 0)\, da/n - P^2$]. Because we mainly consider narrow initial distributions ($\sigma \ll P$), the rain initiation time does not depend substantially on the initial shape. We have checked that using for comparison the more commonly applied Weibull distribution (see Liu and Hallett 1997; Liu et al. 2002) $(\lambda/\sigma)[(a - a_0)/\sigma]^{\lambda-1} \exp\{[(a - a_0)/\sigma]^{\lambda}\}$, for $1 \le \lambda \le 4$. We start from purely gravitational collisions in still air, that is, we solve the space-homogenous version of (1) with no condensation term:

$$\frac{\partial n(a)}{\partial t} = -n(a)\frac{\mathbf{u}_g(a)}{L} + \int da' \left[\frac{K_g(a', a'')n(a')n(a'')}{2(a''/a)^2} - K_g(a', a)n(a')n(a)\right]. \tag{4}$$

The first term in the rhs of (4) models the loss of droplets falling with the settling velocity $\mathbf{u}_g$ from the cloud of the vertical size L. Because L are generally very large (from hundreds of meters to kilometers) and $\mathbf{u}_g(a)$ grows with a (see Fig. 1 below), fallout is relevant only for sufficiently large drops (called raindrops) with sizes of a millimeter or more. The collision (Smoluchowsky) term describes the propagation of distribution toward large sizes. The asymptotic law of propagation depends on the scaling of $K_g(a, a')$. If the collision kernel is a homogeneous function of degree α [i.e., $K_g(\xi a, \xi a') = \xi^{\alpha} K_g(a, a')$], one can show that for α larger (smaller) than 3 the propagation is accelerating (decelerating), while for $\alpha = 3$ it is exponential $\ln a \propto t$ (see van Dongen and Ernst 1988; Zakharov et al. 1992). Our numerics show, however, that the intervals of sizes a where α is approximately a constant are too short for the definite self-similarity of the propagation to form both for narrow and wide initial distributions. This is because of the complexity of both functions $\mathbf{u}_g(a)$ and $E(a, a')$. We thus focus on the most salient feature of the propagation, namely, we study how the amount of liquid water left in the cloud depends on time. Specifically, we study the fraction of water left, $W = \int n(a, t)a^3\, da/\int n(a, 0)a^3\, da$, relative to the value at the beginning. The decrease of that amount is because of a concerted action of collisions producing large drops and fallout.

The droplets radii space was discretized, that is, the droplets size distribution $n(a, t)$ was presented as the set of concentrations $n_i(t)$ of droplets with radius a_i. The grid of radii was taken to be approximately exponential at sizes that are much larger than the size of initial condensation nuclei, with 256 points in the unit interval of the natural logarithm. The collision term in the Smoluchowsky equation was treated as follows: let the radius $(a_i^3 + a_j^3)^{1/3}$ of the droplet resulting from the merging of the two with radii a_i and a_j be in between the two radii a_k and a_{k+1} from the grid. Then, the collision results in decreasing n_i and n_j by the quantity dN that is determined by the collision kernel, while the concentrations n_k and n_{k+1} are increased in such a way that sum of their change is dN and the whole amount of water in droplets is conserved in coalescence:

$$\delta n_i = \delta n_j = -dN = -\delta n_k - \delta n_{k+1},$$
$$a_k^3 \delta n_k + a_{k+1}^3 \delta n_{k+1} = (a_i^3 + a_j^3)dN,$$
$$\delta n_{k+1} = dN(a_i^3 + a_j^3 - a_k^3)/(a_{k+1}^3 - a_k^3),$$

and

$$\delta n_k = dN(a_{k+1}^3 - a_i^3 + a_j^3)/(a_{k+1}^3 - a_k^3). \tag{5}$$

The total amount of water in droplets and that left the cloud was a conserved quantity, up to 10^{-6} accuracy, during the whole simulation. In sections that deal with condensation as well, the conserved quantity is the sum of total mass of vapor, water in droplets, and water that left the cloud. Note that our scheme automatically keeps the numbers positive—if dN is greater than either n_i or n_j, then we choose $dN = \min(n_i, n_j)$, so that n_i and n_j are also not negative after every elementary collision process. Let us stress that our scheme conserves the total mass of water and keeps accurate count of the number of droplets [as compared with the nonconservative scheme of Berry and Reinhardt (1974) and the scheme of Bott (1998), which was conservative only in mass and needed special choice of the time step to keep positivity]. The minimal time step needed for our calculations was estimated from characteristic time scales of our problem to be 0.1 s. We have checked that the decrease of the time step below $dt = 0.05$ s does not change the results; the figures below all correspond to that dt.

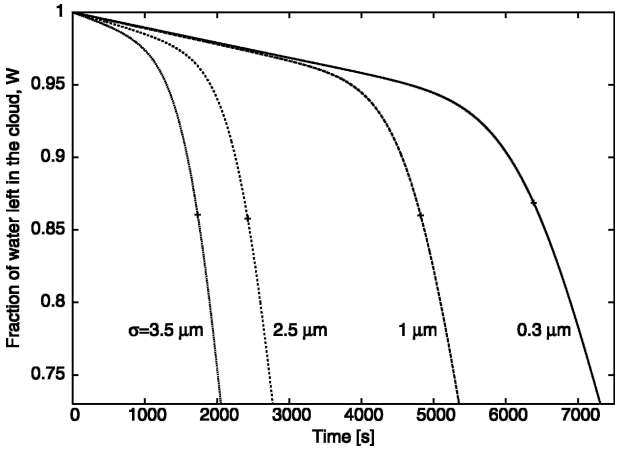

FIG. 2. Fraction of water left in the cloud as a function of time. The mean droplet radius of the initial distribution $n(a)$ is $P = 13$ μm. Different curves correspond to different widths σ of the initial distribution $n(a)$. Fallout of water from the cloud begins with a drizzle, which is later replaced by faster fallout. The moments when this crossover happens are denoted with crosses and represent rain initiation times.

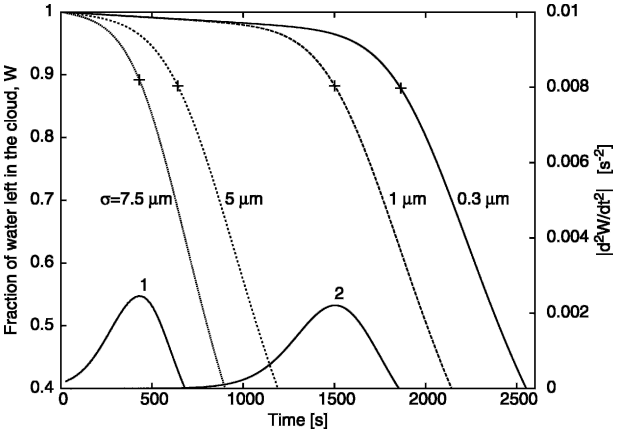

FIG. 3. Fraction of water left in the cloud as a function of time for the mean droplet radius of the initial distribution $n(a)$: $P = 16.7$ μm. Different curves correspond to different widths σ of the initial distribution $n(a)$. Lines 1 and 2 represent the absolute value of the second derivative of fraction of the water left in the cloud for $\sigma = 7.5$ and 1.0 μm, respectively. Fallout of water from the cloud starts with a drizzle, which later is replaced by faster fallout. The moments when this crossover happens are denoted with crosses and represent rain initiation times.

We used the following values of the parameters $\nu = 0.15$ cm^2 s^{-1}, $\rho = 1$ g cm^{-3}, $\rho_0 = 1.2\ 10^{-3}$ g cm^{-3}, and $g = 980$ cm s^{-2}. The graphs $W(t)$ are shown in Figs. 2 and 3 (for $L = 2$ km), and they are qualitatively the same both for narrow and wide initial distributions. At the initial stage, W decreases slowly because of the loss of drizzle. After large raindrops appear, the loss accelerates. At every curve, the star marks the moment when respective $|d^2W/dt^2|$ are maximal (see Fig. 3). After that moment, the cloud loses water fast so it is natural to take t_* as the beginning of rain. Figure 4 shows how the mass distribution over sizes $m(a) \propto a^3 n(a)$ evolves with time (for $P = 16.7$ μm, $\sigma = 1$ μm, $L = 2$ km). One can see the appearance of secondary peaks and distribution propagating to large a. The moment t_* seems to correspond to the highest value of the envelope of the curves $m(a, t)$ of the coalescence-produced drops. One can see from Fig. 4 that the peak at mass distribution is around 200 μm and most of the droplets are below 500 μm at $t = t_*$. The same character of the evolution $W(t)$ can be seen in the next section for the ab initio simulations of (1) and (2).

The rain initiation time t_* defined in that way is presented in Figs. 5 and 6 against the width and the mean radius of the initial distribution. Note the dramatic increase in t_* with decreasing σ for $P = 13$ μm. The mean droplet size $P = 14$ μm is sometimes empirically introduced as the minimal size required for the onset of precipitation (Rosenfeld and Gutman 1994). Figures 5 and 6 support that observation; they indeed show that t_* grows fast when P decreases below that size, but only for very narrow initial distributions, and of course there is no clear-cut threshold as $t_*(P)$ is a smooth (though steep) function. The time scales (from tens of minutes to hours) are in agreement with the data obtained before (see Pruppacher and Klett 1997, chapter 15; Seinfeld and Pandis 1998, chapter 15 and the references therein). Figure 6 also shows that for 15 μm $\lesssim P$, the function $t_*(P)$ can be well approximated by a power law $t_* \propto P^{-\gamma}$ with $\gamma \approx 3$. The rain initiation time depends on the cloud vertical size almost logarithmically as shown in Fig. 7; we do not have an explanation for this func-

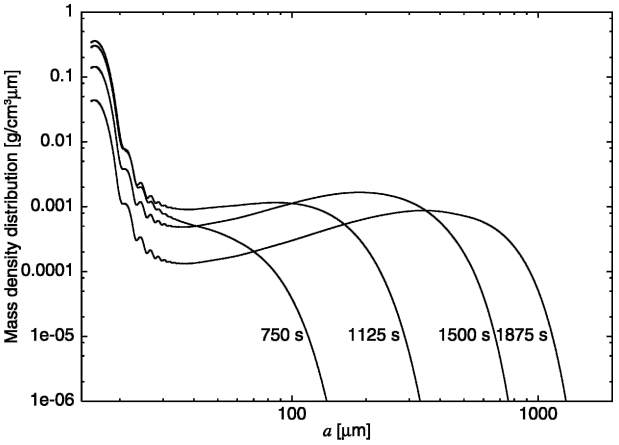

FIG. 4. Mass density of water shown at different moments in time and as a function of droplet radii a. Rain initiation time is $t_* \simeq 1500$ s. Notice how with the evolution of time the largest amount of droplets moves from small radii to larger ones.

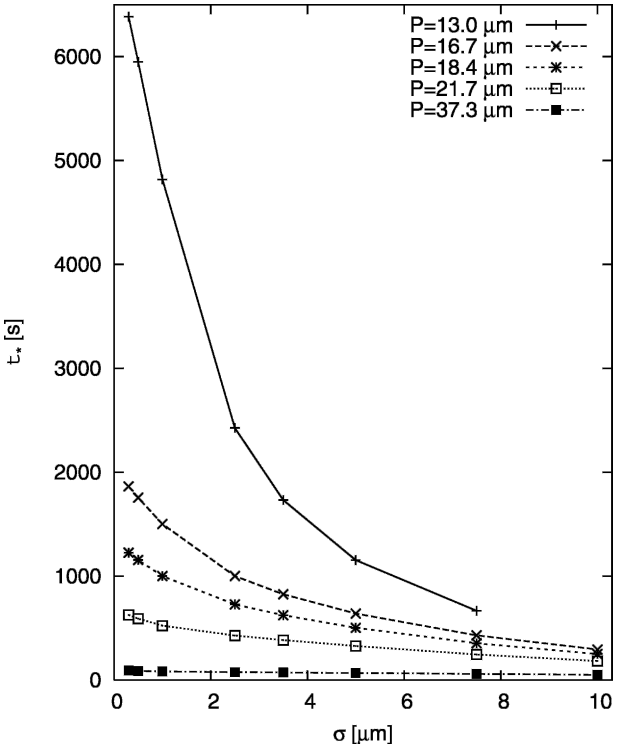

FIG. 5. Rain initiation time as function of the width σ of the initial distribution $n(a)$ for different mean radii P of this distribution. Notice a dramatic increase in t_* with decreasing σ for $P = 13$ μm. The mean droplet radius $P = 14$ μm is empirically introduced as the minimal size required for the onset of precipitation (Rosenfeld and Gutman 1994).

tional form. Let us stress that the dependence on cloud vertical size is given assuming all other parameters are fixed.

Here we treated the position and the width of the distribution as given at the beginning of the collision stage. But, of course, the distribution is itself a product of the condensation stage, so we now turn to the consideration of the full condensation–collision model.

3. Condensation and collisions

We consider now the space-homogeneous system

$$\frac{\partial n(a)}{\partial t} = -\frac{\kappa s M}{\rho_0}\frac{\partial}{\partial a}\frac{n(a)}{a} - n(a)\frac{u_g(a)}{L} + \int da'\left[\frac{K(a', a'')n(a')n(a'')}{2(a''/a)^2} - K(a', a)n(a')n(a)\right] \tag{6}$$

and

$$\frac{\partial M}{\partial t} = -4\pi s M \kappa \int a n(a)\, da. \tag{7}$$

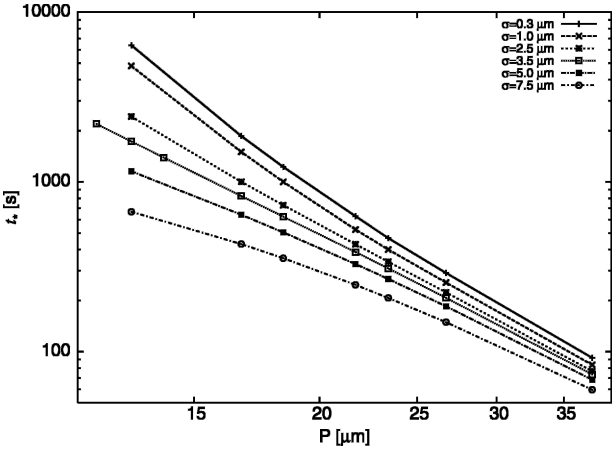

FIG. 6. Rain initiation time as function of the mean radius P of the initial distribution $n(a)$ for different widths σ of this distribution.

The system made up of (6) and (7) is our mean-field model where the only memory of spatial inhomogeneities is the fallout term. Without this term, it has a form of balance relations preserving the total water content (vapor plus droplets) $W_T(t) = M(t) + 4\pi\rho_0 \int n(a, t)a^3\, da/3$. As we show here, this model gives the rain initiation times with reasonable quantitative values and proper qualitative behavior upon the change of parameters. Let us discuss first how t_* depends on the CCN number $n_0 = \int n(a, 0)\, da$. Here, the most important feature is the existence of the minimum in the function $t_*(n_0)$. That can be explained by the competition between condensation, collision, and vapor depletion. Because condensation slows down and coalescence accelerates as the size of droplets grow, there exists a cross-

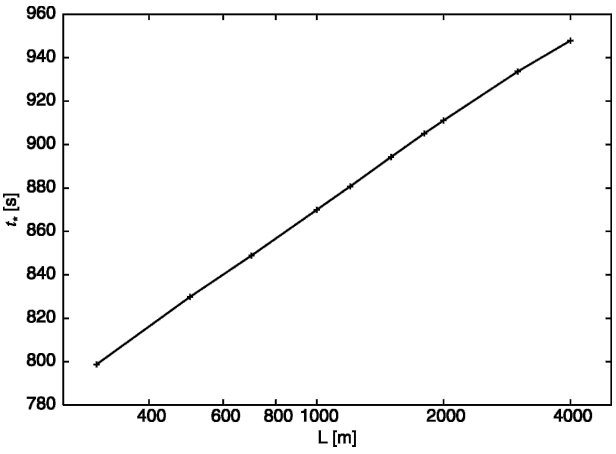

FIG. 7. Rain initiation time as function of the cloud vertical size L for the mean droplet radius $P = 18.8$ μm and the width $\sigma = 1$ μm) of the initial distribution $n(a)$.

over size a_c. With a certain degree of simplification, one can say that the growth until a_c is because of condensation and after that is because of collisions.

Because collisional growth accelerates with the size, an order-of-magnitude estimate for the rain initiation time is the time of condensational growth until a_c. When the CCN number is low enough it does not influence condensation, yet the collisions are more frequent for a higher number of droplets. That means that by increasing n_0 from low values we decrease the crossover size a_c (collisions take over earlier) and thus decrease the time needed for droplet growth. Such a decrease of t_* with n_0 must go until we consider the CCN number, which is large enough for vapor depletion to play a role. Vapor depletion starts to affect condensation when the amount of water in droplets is getting comparable to that in vapor, which corresponds to the droplet size $a_d \simeq (M/n_0\rho_0)^{1/3}$. When droplets grow comparable to a_d vapor depletion slows and then stops condensation. The question now is which size, a_c or a_d, decays faster with n_0. Let us give a rough estimate for a_c. Collisions change the concentration $n(a)$ on a time scale of the order of $1/\int K(a, a_1)n(a_1)\, da_1$. Assuming that during the growth until a_c the total number of droplets did not change much (because condensation was the leading mechanism) and that all droplets have comparable sizes, we get a_c determined by the implicit relation $K(a_c)n_0 \simeq \kappa s M/\rho_0 a_c^2$. Note that for all mechanisms of collision (Brownian, gravitational, and turbulent) the collision kernel $K(a)$ grows faster than a^2 so that a_c decreases with n_0 slower than $n_0^{-1/3}$. That means that for sufficiently small n_0, $a_d > a_c$ and vapor depletion is indeed irrelevant. However, for sufficiently high n_0, a_c is getting comparable to a_d and the decrease of t_* with n_0 stops. If one takes the initial concentration even larger so that $a_c > a_d$, then vapor depletion stops condensation earlier than sizes reach a_c; collisions are slower for droplets of smaller sizes so that the overall time of droplet growth is getting larger. The concentration n_c that corresponds to the minimal time can be found from the (implicit) relation $a_d \simeq a_c$:

$$(M/n_c\rho_0)^{-1/3} K[(M/n_c\rho_0)^{1/3}] \simeq \kappa s. \tag{8}$$

That tells that $n_c \propto M$, and if the kernel is homogeneous $K \propto a^\alpha$, then $n_c \propto s^{3/(1-\alpha)}$. One can argue that for small concentrations (generally for maritime clouds), $n_0 < n_c$, the times of condensation and collision stages are comparable. Therefore, t_* is a function of the product Ms. For a homogeneous kernel, $t_* \propto n^{-2/(2+\alpha)}(Ms)^{-\alpha/(2+\alpha)}$. For large concentrations (generally for continental clouds), $n_0 > n_c$, the rain initiation time is mainly determined by collisions, so it becomes independent of the supersaturation and $t_* \propto n_0^{(\alpha-3)/3} M^{-\alpha/3}$.

Let us illustrate now the nonmonotonic dependence of the rain initiation time of the CCN number by numerically solving (6) and (7). In the effective kinetic model of McGraw and Liu (2003, 2004) the barrier-crossing rate was observed to increase with CCN and then decrease after some value. We substitute $K = K_g$ and start from CCN (i.e., initial droplets) uniformly distributed between 1 and 2 μm. We take $\kappa = \kappa_T = 0.25$ cm^2 s^{-1}, $T = 300$ K, L $= 4\ 10^4$ J mol^{-1}, and $R = 8.3$ J mol^{-1} K. We obtain the rain initiation time (defined by the maximum of d^2W_T/dt^2) as a function of the CCN concentration n_0 for different values of the supersaturation s and the vapor content M. The grid of radii was approximately exponential at sizes that are much larger than the size of initial condensation nuclei (with 200 points in unit interval of natural logarithm). The distribution of water between grid points because of collisions goes according to (5) (the mass of water was conserved and the number of droplets changes in the proper way). The condensation of vapor was taken into account by working on an evolving grid of radii $a_i(t)$, keeping conserved the total mass of water in droplets and vapor. Collisions were modeled according to (5) described above. Note that the numerical scheme we employ here has an additional advantage [when compared with those described in Pruppacher and Klett (1997), Berry and Reinhardt (1974), and Bott (1998)] of accounting simultaneously for condensation and collisions while respecting conservation laws. We used the time step $dt = 0.01$ s during the condensation phase; on a later stage (dominated by coalescence) $dt = 0.1$ s was enough. The same grid is used for condensation and coalescence.

Those results are presented in Fig. 8 for $L = 1$ km. The solitary point at the lower part corresponds to $M = 6$ g m^{-3}, $s = 1/60$. The three solid lines correspond to $M = 3$ g m^{-3} and, respectively, to $s = 0.0173$, 0.0086, 0.0043, from bottom to top. The three dashed lines correspond to $M = 1.5$ g m^{-3} and, respectively, to $s = 0.0196$, 0.0076, 0.0038, from bottom to top.

We see that indeed the graphs $t_*(n_0)$ all have minima. The position of the minimum is proportional to M as expected and approximately proportional to $s^{-1/2}$, which would correspond to $\alpha \simeq 7$ in this interval of sizes. We see that the left parts of different curves with the same value of the product sk approach each other as n decreases. Indeed, the middle dashed line and upper solid line correspond to $k = 4\ 10^{-9}$ cm^2 s^{-1}, while the lower dashed line and middle solid

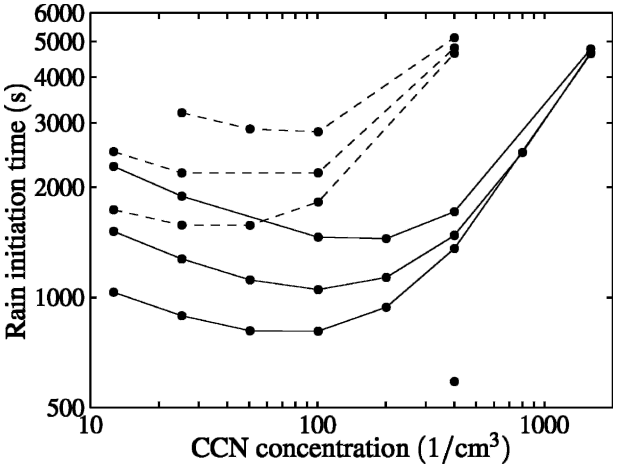

FIG. 8. Rain initiation time t_* as function of CCN concentration n_0 for different values of supersaturation s and water vapor density M. Notice that all $t_*(n_0)$ functions have a minimum. The characteristic cloud size is $L = 1$ km.

line have $k = 2\ 10^{-9}$ cm^2 s^{-1}. To the right of the minima, the curves with different s but the same M approach each other as n increases. That supports the previous conclusions on the respective roles of condensation and collisions in determining the rain initiation time.

Note that the ascending parts of the curves (growth of t_* with n_0), together with Fig. 6, correspond to the so-called second aerosol indirect effect (Squires 1958). Being interested in the qualitative (nonmonotonic) dependence $t_*(n)$ we disregarded here the turbulence contribution into the collision rate (see, e.g., Saffman and Turner 1956; Maxey 1987; Squires and Eaton 1991; Sundaram and Collins 1997; Shaw et al. 1998; Reade and Collins 2000; Grits et al. 2000; Vaillancourt and Yau 2000; Kostinski and Shaw 2001; Falkovich et al. 2002; Falkovich and Pumir 2004; Collins and Keswani 2004; Wang et al. 2005; Franklin et al. 2005 and the references therein). For the parameters considered here, turbulence with the rms velocity gradient $\lambda \leq 15$ s^{-1} can only slightly diminish t_* and cannot change the qualitative form of the dependence $t_*(n)$ (the details will be published elsewhere). We also disregard the regular vertical inhomogeneity of the supersaturation resulting from the temperature profile, which does not broaden $n(a)$ much even with the account of turbulence-induced random fluctuations (Korolev 1995; Turitsyn 2003). Spatial inhomogeneities in vapor density M resulting from the mixing of humid and dry air remain a controversial subject (see, e.g., Pruppacher and Klett 1997; Baker et al. 1980) and probably can be neglected in cloud cores. We address the turbulent mixing of vapor in section 4 considering partially seeded clouds.

4. Delaying rain by hygroscopic overseeding

That the rain time is a nonmonotonic function of the concentration of droplets may provide a partial explanation for the conflicting observations of the effect of hygroscopic seeding. By seeding clouds with hygroscopic aerosol particles one can vary the number of cloud condensation nuclei and thus the number of small droplets at the beginning of the cloud formation. It was observed that such seeding in some cases suppresses precipitation (see, e.g., Rosenfeld et al. 2001), while in other cases it enhances and accelerates it (Cotton and Pielke 1995; Mather 1991; see also Bruintjes 1999 for a recent review).

It is often desirable to postpone rain, for instance, to bring precipitation inland from the sea. The fact that t_* grows when $n_0 > n_c$ suggests the idea of overseeding to delay rain. This is considered to be unpractical: "It would be necessary to treat all portions of a target cloud because, once precipitation appeared anywhere in it, the raindrops . . . would be circulated throughout the cloud . . . by turbulence" (Dennis 1980). We think that this conclusion ignores another, positive, aspect of cloud turbulence, namely, the mixing and homogenization of partially seeded cloud during the condensation stage. Let us describe briefly how it works for two cases.

Consider first seeding a part of the cloud comparable to its size L_c. Note that we do not consider here adding ultragiant nuclei, we assume seeded CCN to be comparable in size to those naturally present. According to the Richardson law, the squared distance between two fluid parcels grows as εt^3 so that the rms difference of vapor concentrations between seeded and unseeded parts decreases as $t^{-9/4}$ when $t^3 > t_0^3 = L_c^2/\varepsilon$ (ε is the energy dissipation rate in turbulence). To see how different rates of condensation interplay with turbulent mixing we generalize the mean field system [(6) and (7)] describing seeded and unseeded parts by their respective n_1, n_2 and $x_1 = s_1 M_1$, $x_2 = s_2 M_2$, and link them by adding the term that models the decay of the difference, $dx_i/dt = \ldots - (x_i - x_j)t(t + t_0)^{-2}(9/4)$. As a crude model, we assume the two parts evolve separately until $t = 2t_0$, then we treat the cloud as well mixed and allow for the collisions between droplets from different parts. This actually underestimates the effect of seeding and can be considered as giving the lower bound for the time before rain. The results of simulations are shown in Fig. 9 for $t_0 = 180$ s, $L = 1$ km, and $\lambda = 15$ s^{-1}. It is seen from Fig. 9a that the total water content W_T changes similarly to what was shown in Figs. 2 and 3, and the rain initiation time is again determined by the maximum of d^2W_T/dt^2. The respective times are shown against $n_0 = (n_1 + n_2)/2$ by boxes in

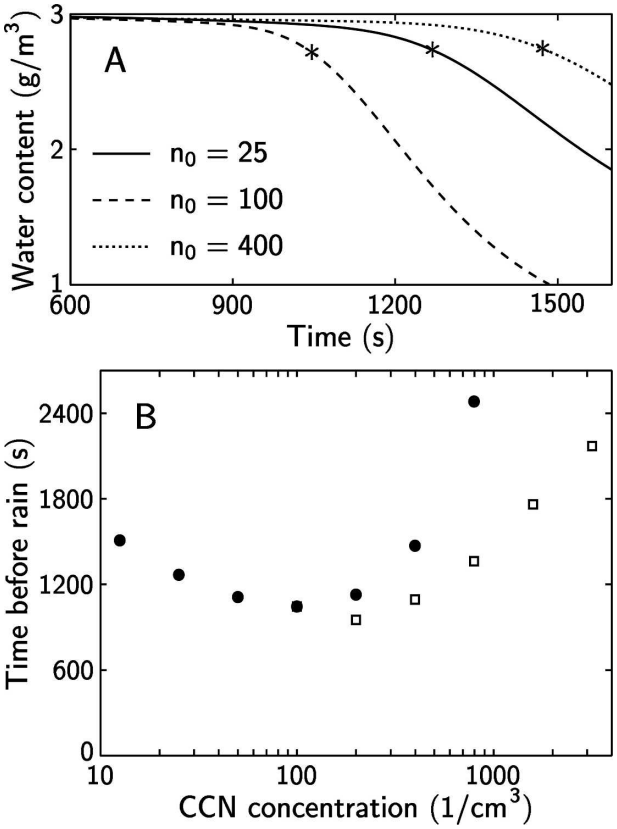

FIG. 9. (a) Fraction of water left in the cloud as a function of time. The asterisk signs mark rain initiation times t_*, which are times at which the slow drizzle fallout of water from the cloud is replaced by a more rapid one. (b) Rain initiation time t_* as a function of CCN concentration n_0. The lower part (boxes) corresponds to a half-seeded cloud (the half-sum of concentrations is used as abscissa) while the upper part (filled circles) corresponds to an unseeded one. The time increase for a half-seeded cloud is less than that for a homogeneously seeded one, but it is still substantial. Notice that seeding a bit can accelerate rain, but taking, e.g., $n_1 = 100$ cm^{-3} and seeding with $n_2 \simeq 3000$ cm^{-3} would cause a postponement of rain of about 10 min.

Fig. 9b. The time increase is less than that for homogeneous seeding but is still substantial. The fraction of the cloud still unmixed after time t decreases by the Poisson law $\exp(-t/t_0)$. Taking $n_1 = 100$ cm^{-3} one sees that for a time delay of 10 min one needs to seed by $n_2 \simeq 3000$ cm^{-3}.

Second, consider seeding by N particles a small part of the cloud that (unseeded) had some n_0 and would rain after t_*. After time t_* the seeds spread into the area of size $(\varepsilon t_*^3)^{1/2}$ with the concentration inside the mixed region decaying as $n(t_*) = N(\varepsilon t_*^3)^{-3/2}$ [for stratiform clouds one gets $N(\varepsilon t^3)^{-1}$]. To have an effect of seeding, one needs $n(t_*) > n_0$, which requires $N > 10^{15}$ for $n_0 = 50$ cm^{-3}, $t_* = 10$ min, and $\varepsilon = 10$ cm^2 s^{-3}; with submicrometer particles weighing 10^{-11} g that would mean hundreds of kilograms, which is still practical.

5. Summary

We believe that our main result is a simple mean field model [(6) and (7)] that demonstrates nonmonotonic dependence of the rain initiation time on CCN concentration. As the CCN concentration increases, the rain initiation time first decreases and then grows as shown in Figs. 8 and 9. The simple modification of this model for an inhomogeneous case described in section 4 shows that one can increase the rain initiation time even for a cloud that is partially seeded by hygroscopic aerosols.

Acknowledgments. We acknowledge support by the Ellentuck fund, by the Minerva Foundation, and by NSF under Agreement DMS-9729992. The work has been supported by the European research network and Israel Science Foundation. Authors GF and MS thank the Aspen Center for Physics for their hospitality. We are grateful to A. Khain, M. Pinsky, and D. Rosenfeld for useful discussions and to the referees for helpful suggestions.

REFERENCES

Baker, M. B., R. G. Corbin, and J. Latham, 1980: The effects of turbulent mixing in clouds. *Quart. J. Roy. Meteor. Soc.,* **106,** 581–598.

Beard, K. V., R. I. Durkee, and H. T. Ochs, 2002: Coalescence efficiency measurements for minimally charged cloud drops. *J. Atmos. Sci.,* **59,** 233–243.

Berry, E. X., and R. L. Reinhardt, 1974: An analysis of cloud drop growth by collection: Part I. Double distributions. *J. Atmos. Sci.,* **31,** 1814–1824.

Bott, A., 1998: A flux method for the numerical solution of the stochastic collection equation. *J. Atmos. Sci.,* **55,** 2284–2293.

Bruintjes, R. T., 1999: A review of cloud seeding experiments to enhance precipitation and some new prospects. *Bull. Amer. Meteor. Soc.,* **80,** 805–820.

Collins, L. R., and A. Keswani, 2004: Reynolds number scaling of particle clustering in turbulent aerosols. *New J. Phys.,* **6,** 119, doi:10.1088/1367-2630/6/1/119.

Cotton, W. R., and R. A. Pielke, 1995: *Human Impacts on Weather and Climate.* Cambridge University Press, 296 pp.

Dennis, A. S., 1980: *Weather Modification by Cloud Seeding.* Academic Press, 267 pp.

Falkovich, G., and A. Pumir, 2004: Intermittent distribution of heavy particles in a turbulent flow. *Phys. Fluids,* **16,** L47–L50.

——, A. Fouxon, and M. G. Stepanov, 2002: Acceleration of rain initiation by cloud turbulence. *Nature,* **419,** 151–154.

Franklin, C., P. Vaillancourt, M. K. Yau, and P. Bartello, 2005: Collision rates of cloud droplets in turbulent flow. *J. Atmos. Sci.,* **62,** 2451–2466.

Grits, B., M. Pinsky, and A. Khain, 2000: Formation of small-scale droplet concentration inhomogeneity in a turbulent flow as seen from experiments with an isotropic turbulence model. *Proc. 13th Int. Conf. on Clouds and Precipitation,* Reno, NV, ICCP, 132–134.

Gunn, R., and G. D. Kinzer, 1949: The terminal velocity of fall for water droplets in stagnant air. *J. Meteor.,* **6,** 243–248.

Korolev, A., 1995: The influence of supersaturation fluctuations on droplet size spectra formation. *J. Atmos. Sci.,* **52,** 3620–3634.

Kostinski, A., and R. Shaw, 2001: Scale-dependent droplet clustering in turbulent clouds. *J. Fluid Mech.,* **434,** 389–398.

Liu, Y. G., and J. Hallett, 1997: The "1/3" power law between effective radius and liquid-water content. *Quart. J. Roy. Meteor. Soc.,* **123,** 1789–1795.

——, P. H. Daum, and J. Hallett, 2002: A generalized systems theory for the effect of varying fluctuations on cloud droplet size distributions. *J. Atmos. Sci.,* **59,** 2279–2290.

Mather, G. K., 1991: Coalescence enhancement in large multicell storms caused by the emissions from a Kraft paper mill. *J. Appl. Meteor.,* **30,** 1134–1146.

Maxey, M. R., 1987: The gravitational settling of aerosol particles in homogeneous turbulence and random flow field. *J. Fluid Mech.,* **174,** 441–465.

McGraw, R., and Y. Liu, 2003: Kinetic potential and barrier crossing: A model for warm cloud drizzle formation. *Phys. Rev. Lett.,* **90,** doi:10.1103/PhysRevLett.90.018501.

——, and ——, 2004: Analytic formulation and parametrization of the kinetic potential theory for drizzle formation. *Phys. Rev. E,* **70,** doi:10.1103/PhysRevE.70.031606.

Pinsky, M., A. Khain, and M. Shapiro, 2001: Collision efficiency of drops in a wide range of Reynolds numbers. *J. Atmos. Sci.,* **58,** 742–766.

Pruppacher, H. R., and J. D. Klett, 1997: *Microphysics of Clouds and Precipitation*. 2d ed. Kluwer Academic, 976 pp.

Reade, W., and L. Collins, 2000: Effect of preferential concentration on turbulent collision rates. *Phys. Fluids,* **12,** 2530–2540.

Rosenfeld, D., and G. Gutman, 1994: Retrieving microphysical properties near the tops of potential rain clouds by multispectral analysis of AVHRR data. *Atmos. Res.,* **34,** 259–283.

——, Y. Rudich, and R. Lahav, 2001: Desert dust suppressing precipitation: A possible desertification feedback loop. *Proc. Natl. Acad. Sci. USA,* **98,** 5975–5980.

Saffman, P., and J. Turner, 1956: On the collision of drops in turbulent clouds. *J. Fluid Mech.,* **1,** 16–30.

Seinfeld, J., and S. Pandis, 1998: *Atmospheric Chemistry and Physics: From Air Pollution to Climate Change*. John Wiley and Sons, 1326 pp.

Shaw, R., W. Reade, L. Collins, and J. Verlinde, 1998: Preferential concentration of cloud droplets by turbulence: Effect on early evolution of cumulus cloud droplet spectra. *J. Atmos. Sci.,* **55,** 1965–1976.

Squires, K., 1958: The microstructure and colloidal stability of warm clouds. *Tellus,* **10,** 256–261.

——, and J. Eaton, 1991: Measurements of particle dispersion from direct numerical simulations of isotropic turbulence. *J. Fluid Mech.,* **226,** 1–35.

Sundaram, S., and L. Collins, 1997: Collision statistics in an isotropic particle-laden turbulent suspension. *J. Fluid Mech.,* **335,** 75–109.

Turitsyn, K. S., 2003: Air parcel random walk and droplet spectra broadening in clouds. *Phys. Rev. E,* **67,** 062 102–062 103.

Vaillancourt, P. A., and M. K. Yau, 2000: Review of particle-turbulence interactions and consequences for cloud physics. *Bull. Amer. Meteor. Soc.,* **81,** 285–298.

van Dongen, P. G. J., and M. H. Ernst, 1988: Scaling solutions of Smoluchowski's coagulation equation. *J. Stat. Phys.,* **50,** 295–328.

Wang, L.-P., O. Ayala, S. Kasprzak, and W. Grabowski, 2005: Theoretical formulation of collision rate and collision efficiency of hydrodynamically interacting cloud droplets in turbulent atmosphere. *J. Atmos. Sci.,* **62,** 2433–2450.

Zakharov, V., V. Lvov, and G. Falkovich, 1992: *Kolmogorov Spectra of Turbulence.* Springer-Verlag, 264 pp.